Available online at www.sciencedirect.com
ScienceDirect
Journal of the European Ceramic Society 29 (2009) 2849–2855
www.elsevier.com/locate/jeurceramsoc

Investigation of thermal expansion of 3D-stitched C–SiC composites

Suresh Kumar [a,*], Anil Kumar [a], Anupam Shukla [b], G. Rohini Devi [a], A.K. Gupta [b]

[a] *Advanced Systems Laboratory, DRDO, Hyderabad 500058, India*
[b] *Department of Chemical Engineering IIT Delhi, New Delhi 110016, India*

Received 28 October 2008; received in revised form 25 March 2009; accepted 3 April 2009
Available online 6 May 2009

Abstract

Carbon fiber reinforced silicon carbide (C–SiC) composites are promising materials for a severe thermo-erosive environment. 3D-stitched C–SiC composites were fabricated using liquid silicon infiltration. The infiltration was carried out at 1450–1650 °C for 10–120 min in vacuum. Coefficient of thermal expansion (CTE) of the composites was determined in in-plane and through-thickness directions in the temperature range from room temperature to 1050 °C. The in-plane CTE varies in the range (0.5–2) × 10^{-6}/°C, while that in the through-thickness direction, it varies in the range (1.5–4) × 10^{-6}/°C. The effect of siliconization conditions is higher in the through-thickness direction than in the in-plane direction. The CTE values are lower than the values reported for chemical vapor impregnation based 3D C–SiC composites. An extensive microstructure study was also carried out to understand the thermal expansion behavior of the composites. It was found out that CTE behavior is closely related to the composition of the composite which in turn depends upon siliconization conditions. The best conditions were 1650 °C and 120 min.

Keywords: Composites; Thermal properties; Thermal expansion; 3D-stitched C–SiC

1. Introduction

Liquid silicon infiltration (LSI) process was developed by German Aerospace Centre (DLR) for processing bi-directional (2D) carbon–silicon-carbide (C–SiC) composites.[1] The LSI process is relatively economic and fast as compared to chemical vapor impregnation (CVI) and polymer impregnation processes. Major applications of C–SiC composites include nose tip of reusable space vehicles, leading edges of hypersonic vehicles, jet-vanes for thrust vectoring, and brake discs for high speed automobiles.[2,3] These products require uniform thermal properties in all the directions to meet the thermo-structural loads. Coefficient of thermal expansion (CTE) is an important design input. Many researchers have reported CTE data for LSI based 2D C–SiC composites.[4,5] It is much higher in the through-thickness direction as compared to that in the in-plane direction, which may lead to thermal shock failure.

CTE of 2D C–SiC composites may be improved by introducing carbon fibers in the third direction perpendicular to the fabric. 3D-stitched C–SiC composites are fabricated to achieve a better CTE in all the directions. These have been fabricated using coal-tar pitch as a carbon precursor. CTE depends on reinforcement orientation, composition (carbon-fibers, carbon-matrix, silicon-carbide (SiC) and silicon) and microstructure of the composite. The composition and microstructure of these composites would depend upon siliconization conditions and on the rate of cooling.[6,7] The temperature of silicon infiltration in the carbon performs has been reported to be in the range 1420–1600 °C.[3–6,9] The infiltration time ranges from a few minutes to 2 h depending on the size of the C–C preform.[5,6] CTE of composites can be explained and estimated by the rule of mixtures[8] but for complex fiber architectures estimation is difficult. Therefore, it needs to be determined experimentally.

1.1. Aim and scope of the work

It was decided to fabricate coal–tar pitch carbon precursor based 3D-stitched C–SiC composites which should have very close thermal expansion in the in-plane and in the through-thickness directions.

For this purpose a standard procedure was developed for the preparation of 3D-stitched carbon–carbon (C–C) performs. These C–C preforms were siliconized at two different temperatures (1450 and 1650 °C) and for two different time intervals (10

* Corresponding author. Tel.: +91 40 24306994; fax: +91 40 24306498.
E-mail address: sureshtanwar@rediffmail.com (S. Kumar).

0955-2219/$ – see front matter © 2009 Elsevier Ltd. All rights reserved.
doi:10.1016/j.jeurceramsoc.2009.04.005

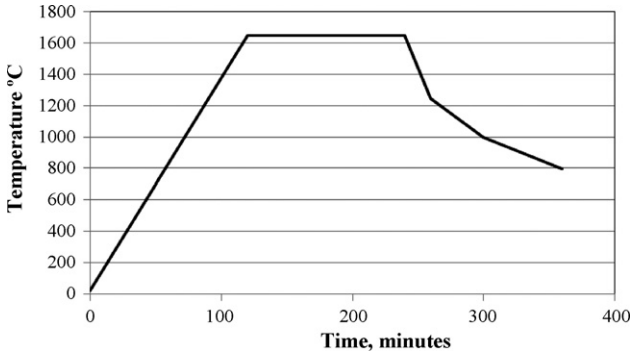

Fig. 1. A typical siliconization cycle for blocks b-7 and b-8.

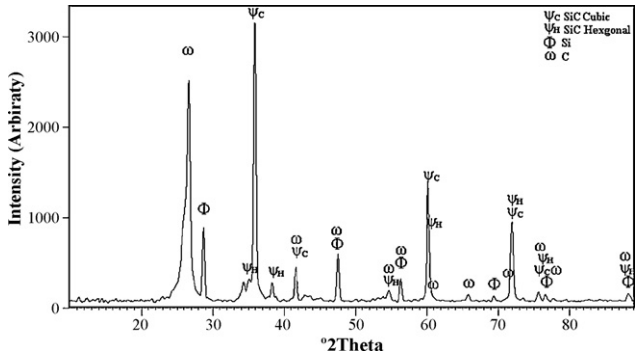

Fig. 2. XRD image of the C–SiC composite block-1.

and 120 min), respectively, to see the effect of temperature and time on siliconization and also on thermal expansion behavior of the composites.

It was also felt necessary to correlate the thermal expansion behavior with the chemical composition and the other characteristics of the composites.

2. Experimental

2.1. Preparation of 3D-stitched C–SiC composites

2.1.1. Raw materials

3k PAN fiber tow based 8H satin fabric having 24 ends per inch and an average thickness of 0.45 mm was used for making the preforms. PAN based 6k carbon–fiber tows were used for stitching. Indigenously available coal–tar pitch having softening point between 85 and 120 °C and coking value 45–50% was used as a carbon precursor. Indigenously available silicon metal of purity >98% was used for siliconization.

2.1.2. Procedure

Fibrous preforms were prepared by stitching several layers of carbon fabric by carbon–fiber tows. Number of stitches was maintained in the range 350–400 per 100 cm^2. The preforms were rigidized by vacuum infiltration of coal–tar pitch at 200–300 °C followed by carbonization at 900–1000 °C, and graphitization at 2400–2600 °C in the nitrogen atmosphere. The rigidized preforms were further densified by a hot-isostatic-pressure-impregnation-carbonization (HIPIC) process at 800 °C and 1000 bar. These were termed as C–C performs; their density was found to lie in the range 1.55–1.60 g/cm^3. Some of these blocks were cut to obtain eight different blocks of sizes 75 mm × 50 mm × 20 mm to 150 mm × 50 mm × 50 mm and were named b-1 to b-8. These eight blocks were siliconized at four siliconization conditions to obtain 3D C–SiC composites: b-1 and b-2 were siliconized at 1450 °C for 10 min, b-3 and b-4 at 1450 °C for 120 min, b-5 and b-6 at 1650 °C for 10 min, and b-7 and b-8 were siliconized at 1650 °C for 120 min. A representative heating and cooling cycle for blocks b-7 and b-8 is shown in Fig. 1. The specific siliconization conditions were arrived at keeping in mind the process requirements and the siliconization furnace limitations.

2.2. Analysis

The C–SiC composites were analyzed: (i) by XRD to determine phases present; (ii) chemical composition was determined by acid digestion method; (iii) pore structure and porosity were determined by mercury porosimetry; (iv) microstructure by optical and scanning electron microscopy; (v) CTE was determined by dilatometer.

2.2.1. XRD analysis

XRD was carried out for all the composite blocks. A representative XRD pattern of b-1 is shown in Fig. 2. The patterns were similar in all the blocks. The results of the XRD studies will be discussed later.

2.2.2. Chemical composition determination

The composite blocks contain carbon fibers and un-reacted carbon matrix, SiC, and residual silicon. The un-reacted carbon fibers and carbon matrix were considered as C–C. Relative

Table 1
Density and composition of the C–SiC composite blocks after siliconization.

S. No.	Temp., °C	Time, min	C–C perform density, g/cm^3	C–SiC density, g/cm^3	Open porosity, %	C–C, wt/wt	SiC, wt/wt	Silicon, wt/wt
b-1	1450	10	1.58	2.19	4.86	0.568	0.335	0.097
b-2	1450	10	1.59	2.19	4.81	0.592	0.335	0.073
b-3	1450	120	1.60	2.33	3.71	0.538	0.359	0.102
b-4	1450	120	1.60	2.30	3.68	0.530	0.359	0.111
b-5	1650	10	1.59	2.23	5.31	0.582	0.348	0.069
b-6	1650	10	1.58	2.17	5.29	0.599	0.348	0.053
b-7	1650	120	1.59	2.19	5.42	0.563	0.384	0.053
b-8	1650	120	1.60	2.20	5.46	0.559	0.384	0.057

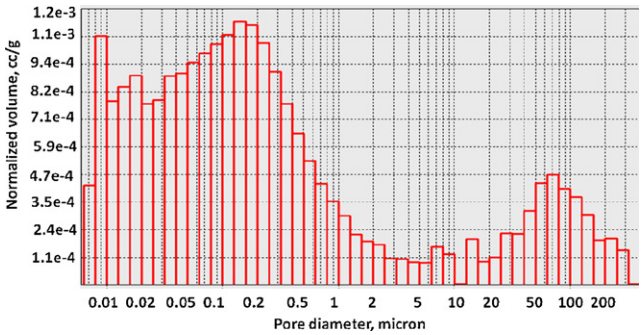

Fig. 3. Pore size distribution of C–SiC composite siliconized at 1450 °C, 120 min.

amount of each was determined by chemical analysis. A small mass of each composite block was powdered. About 5 g powder was digested in 50 ml acid mixture ($HF:HNO_3$, 4:1) for 24 h. Silicon in the composite powder dissolved in the acid. The residue (carbon and SiC) was obtained by filtering the solution. Mass of SiC was determined by heating the residue in air at about 600 °C thus burning off the carbon.[9,10] Composition of all blocks is given in Table 1.

2.2.3. Pore structure determination

Pore size distribution and porosity studies were carried out by mercury porosimetry using Quantachrome instrument. Pore structure of all the specimens was similar. A representative pore size distribution is shown in Fig. 3. Porosity values of all the blocks are given in Table 1. The results are discussed in Section 3.1.

2.2.4. CTE determination

Several test specimens of diameter 6 mm and length 25 mm were cut in in-plane (or parallel) and through-thickness (T-T) directions from the composite blocks (b-1 to b-8). The configuration of the specimens is shown in Fig. 4. CTE measurements were conducted in nitrogen atmosphere, from room temperature to 1050 °C using DIL 402C Dilatometer (NETZSCH Germany). Temperature of the specimens was raised at the rate of 5 °C/min. The change in the specimen length (resulting due to temperature rise) was measured. The coefficient of the linear thermal expansion was calculated as $CTE = (\Delta L/L)/\Delta T$; where $\Delta L/L$ is the fractional change in length of the specimen due to temperature change ΔT.

2.2.5. Microstructure analysis

Microstructure studies were carried out for all the blocks with the help of an optical microscope and also a scanning electron microscope (SEM) to understand the effect of siliconization conditions. A few representative optical and SEM images of blocks siliconized at different conditions are shown in Fig. 5. Similar microstructures were observed for all the blocks. However, the distribution of un-reacted silicon, SiC and carbon was somewhat different, i.e. residual silicon was observed highest in block b-1 while it the least in the block b-8. Discussion about the microstructure is given Section 3.2.

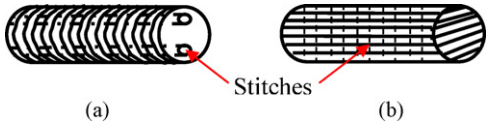

Fig. 4. Configuration of test specimens for CTE determination: (a) through-thickness (T-T) and (b) in-plane (or parallel).

3. Results and discussion

3.1. Effect of siliconization conditions on composition and other characteristics

XRD images show three phases, viz., β-SiC, carbon, and silicon (Fig. 2), all the three phases were present in all the composite blocks. It is evident that the infiltrated silicon reacts with the carbon matrix and forms silicon carbide. However the infiltrated silicon is not fully converted to SiC. Therefore SiC, carbon, and residual silicon are present in all the composite blocks.

Pore size varies in the range 0.001–380 μm in all the composite blocks: however pores below 1 μm diameter account for about 80% of the total pore volume. Open porosity was found to be in the range 3.68–5.46%. It was the least in the blocks b-3 and b-4 and the highest in the blocks b-7and b-8.

The density of the composite blocks varies in the range 2.19–2.33 g/cm^3 (Table 1). It is the highest for the blocks b-3 and b-4 (1450 °C and 120 min) and the least for blocks b-7 and b-8 (1650 °C and 120 min). Porosity and density are closely related to each other.

Chemical composition of all the composite blocks was also determined. SiC fraction was the highest in the blocks b-7 and b-8 (1650 °C, 120 min) and the least in the blocks b-1 and b-2 (1450 °C, 10 min). SiC fraction increased with siliconization time and temperature. The un-reacted silicon was the highest in the blocks b-3 and b-4 and the least in the blocks b-7 and b-8. The un-reacted silicon increases with time at 1450 °C; it decreases with time at 1650 °C. These observations indicate that the rate of formation of SiC is much slower as compared to the rate of infiltration of silicon.

It may be inferred that chemical composition and hence all the other characteristics are governed by siliconization conditions.

3.2. Microstructure studies

Two different types of microstructures are observed in all the blocks: (i) carbon is surrounded by the SiC and (ii) SiC crystals are embedded in the residual silicon. There is no evidence of SiC formation at the carbon fiber surface. Similar microstructures have also been reported in literature.[11,12]

Micro-cracks were observed in the matrix of all the composite blocks: the cracks are mainly in the direction perpendicular to that of the carbon fibers. The cracks in the blocks would have developed due to thermal expansion-mismatch of the residual silicon and the carbon fibers during cooling after siliconization. Had the cracks been present before siliconization, those

would have been filled by the molten silicon during siliconization. It is reported that the initial formation of SiC layer is very fast, and its subsequent growth is controlled by diffusion of silicon through it. There is a volume misfit between carbon and the product SiC[13]. Therefore, some of the SiC formed may break into small particles and move to liquid silicon pool. It is also evident that the carbon fibers remain unaffected by siliconization (Fig. 5e and f). The fibers are surrounded by graphitic carbon, which protects the carbon fibers from the carbon–silicon reaction.

3.3. Coefficient of thermal expansion

CTE of the composite would depend on the CTEs of individual constituents, viz., carbon fibers, carbon matrix, SiC and residual silicon. CTE of silicon and SiC are very close and have been reported to be in the range (4–6) $\times 10^{-6}/^{\circ}C$[14] and (3–5.1) $\times 10^{-6}/^{\circ}C$, respectively.[15–18] C–C composites show anisotropic CTE. For coal–tar pitch based 2D C–C composites it is reported to be in the range (0–0.27) $\times 10^{-6}/^{\circ}C$ in the in-plane direction while (3.0–9.1) $\times 10^{-6}/^{\circ}C$ in the through-thickness

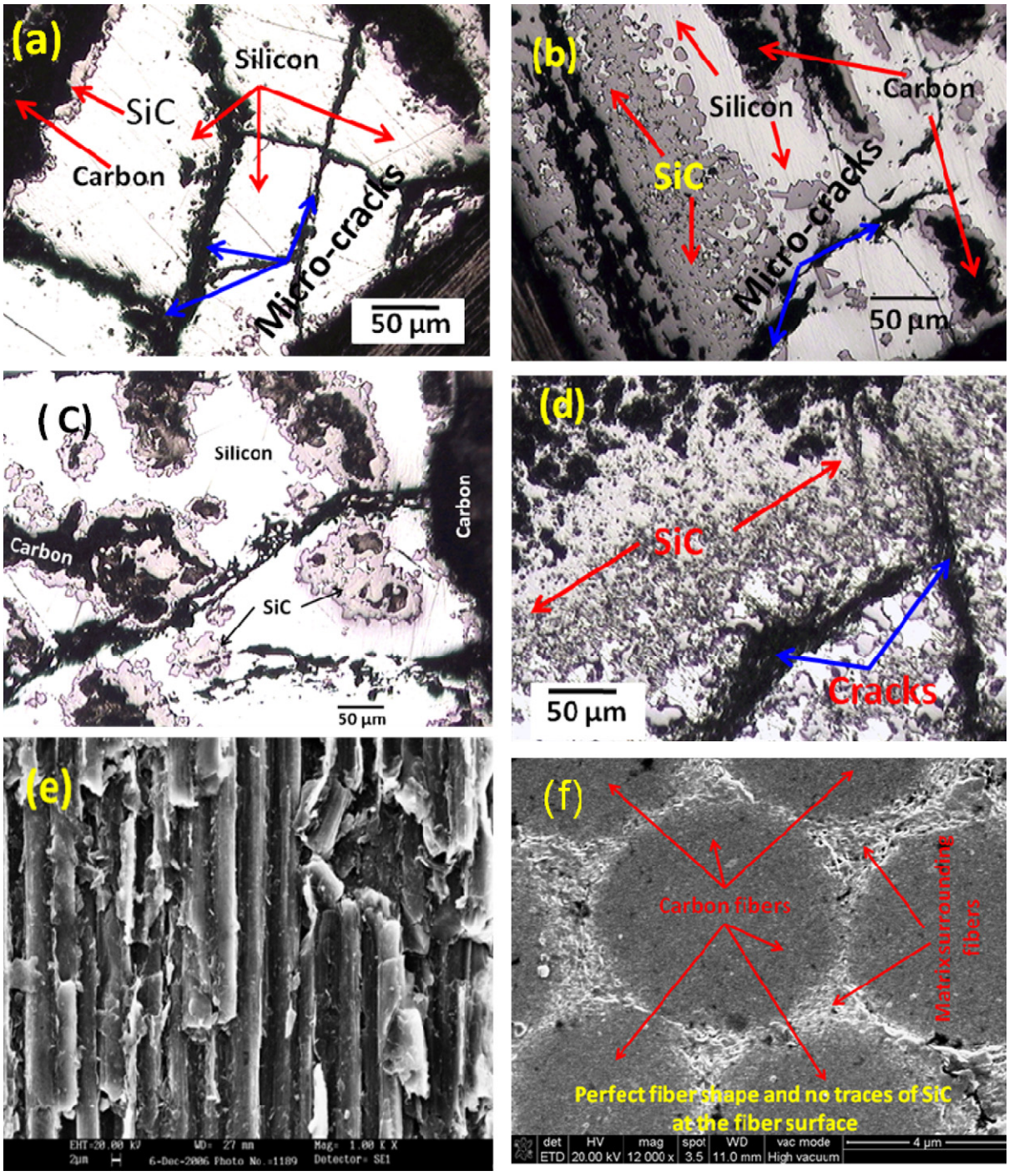

Fig. 5. Microstructures of C–SiC composites processed at different conditions: (a) block-1, (b) block-3, (c) block-5 and (d–f) block-8.

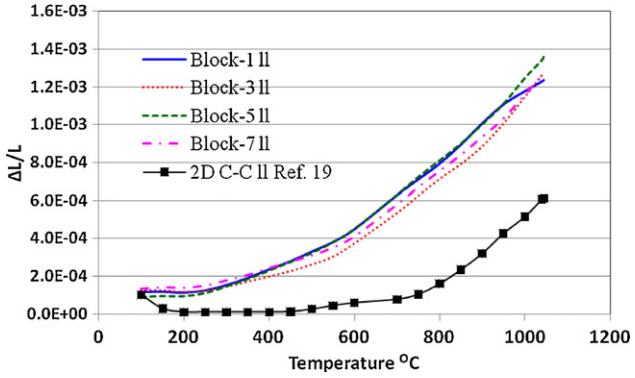

Fig. 6. Relationship between in-plane linear expansion and temperature.

direction.[19] The expansion of the PAN based carbon fibers treated at 2800 °C is negative below 400 °C, and positive at temperatures higher than 400 °C[20,21]. It varies from -1×10^{-6}/°C at 150 °C to 1.5×10^{-6}/°C at 1000 °C[21]. Also, CTE of such composites is affected by the thermal-treatment history and the rate of cooling.

3.3.1. Expansion in the in-plane direction

In the present study expansion was measured for four blocks b-1, b-3, b-5 and b-7 (Fig. 6). It is very similar in all the four blocks in spite of the variation in their chemical composition. The fiber architecture of these blocks in in-plane direction is very similar to that of the 2D C–C composites[19]. Therefore expansion of the above composite blocks has been compared with that of a 2D C–C composite in the same figure.

It is evident that the expansion of 3D-stitched composites is more than that for 2D C–C composite over the entire temperature range. The expansion is small up-to 600 °C and relatively higher at higher temperatures.

For quantitative comparison, the thermal expansion data were well correlated by straight line equations in two temperature segments; (1) between 100 and 600 °C and (2) between 600 and 1050 °C (Fig. 7).

In segment-1, expansion of the 2D C–C composite is almost zero while that of C–SiC composite blocks is $5 \times 10^{-7} T + 5 \times 10^{-5}$, where T is the temperature in °C. In segment-2, expansion of 2D C–C composites is $1 \times 10^{-6} T$ while expansion of C–SiC composite blocks is

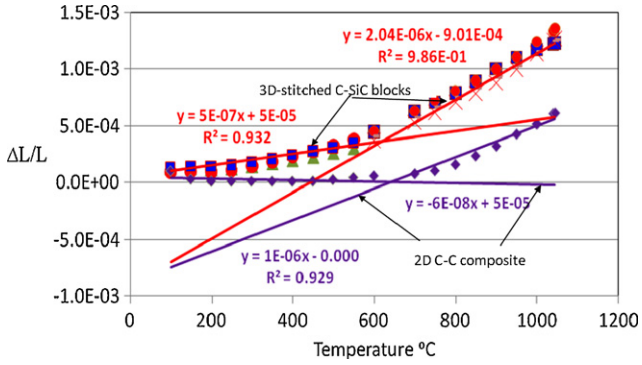

Fig. 7. Thermal expansion comparison of 2D C–C and C–SiC.

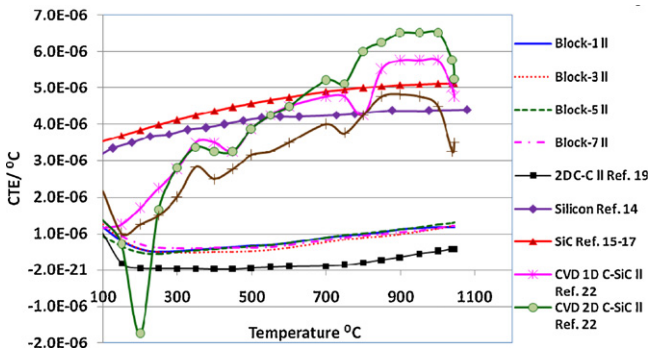

Fig. 8. Relationship between in-plane CTE and temperature.

$2.04 \times 10^{-6} T - 9 \times 10^{-4}$. It shows that the expansion of the C–SiC composite blocks is about twice that of 2D C–C composites at entire temperature range.

3.3.2. CTE

From the $\Delta L/L$ vs. temperature data, CTE was calculated and compared with the values of (a) constituents of the C–SiC composites reported in the literature, with 2D C–C composite and with CTE's of CVD based C–SiC composites (Fig. 8).

CTE is about 1.25×10^{-6}/°C for all the blocks in the present study, it is fairly close to that of PAN based carbon fibers as mentioned earlier. It is much lower than that for silicon as well as SiC. It is also lower than that for CVD based 1D and 2D C–SiC. However, the CTE of C–SiC composite blocks is always higher than that of 2D C–C composite. They decrease in both the cases up to 250 °C. The values are almost constant between 250 and 650 °C. Beyond 650 °C, both increase marginally.

The observed reduction in CTE up to 250 °C may be due to: (i) the expansion is absorbed by the micro-cracks and (ii) negative expansion (or contraction) of carbon fibers in this temperature range.[19]

(1) During siliconization the C–C blocks get filled with molten silicon. Some part of the silicon gets converted into SiC while the remaining is present as such into the pores of the blocks. SiC and the residual silicon shrink uniformly during cooling. Silicon is brittle as compared to SiC and carbon fibers. The matrix of the C–SiC composite blocks experiences thermal stress due to CTE mismatch which results into micro-cracks in the residual silicon (Fig. 5(a–d)). A low expansion in the temperature range 100–300 °C shows that the thermal stresses are released and the micro-cracks get filled.

(2) As shown in Fig. 4b, the direction of the thermal expansion measurement is parallel to the axis of warp fibers and axis of the weft fibers is in perpendicular direction. Third direction fibers hold the stack of the fabrics together. Volume fraction of the third direction carbon fibers is about 0.07 of total reinforcement. Carbon-fibers shrink more in the radial direction and negligibly along the axis.[19,20] The expansion of the composite blocks in the axial direction is mainly controlled by the expansion of the warp carbon-fibers as it the least among all the constituents of C–SiC composites. Therefore

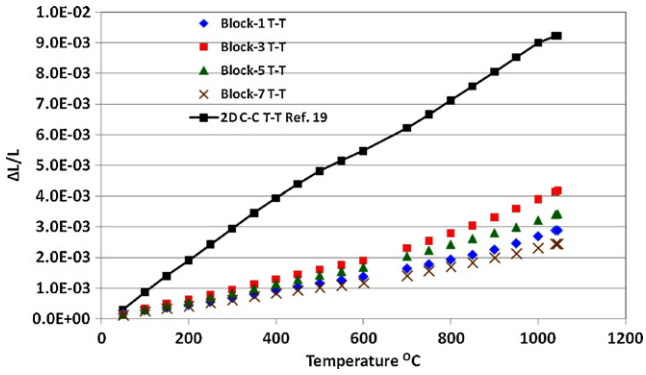

Fig. 9. Relationship between through-thickness expansion and temperature.

CTEs of the C–SiC composite blocks are very low. CTEs of all the blocks are similar because volume fraction of the warp fibers is same in all the blocks.

Thus, the effect of the siliconization conditions on CTE is almost negligible.

3.3.3. Through-thickness (T-T) expansion

Expansion of the blocks b-1, b-3, b-5, b-7 and 2D C–C composite in through-thickness direction is shown in Fig. 9. For all the blocks expansion is much less than that for 2D C–C composites.

It is evident that the siliconization conditions have a strong effect on the expansion. Block-3 (1450 °C, 120 min) shows the maximum expansion, whereas block-7 (1650 °C, 120 min) shows the least expansion.

The expansion of block b-7 has been compared quantitatively with that for 2D C–C composite (Fig. 10).

As in the case of in-plane expansion through-thickness expansion may also be understood in two temperature segments: (i) 100–600 °C, and (ii) 600–1050 °C. The expansion is less in the segment-1 as compared to that in the segment-2. The expansion of the 2D C–C composite is about 4 times higher than that of b-7 in segment-1 and about 3 times higher in segment-2.

3.3.4. CTE

As in the case of in-plane expansion, CTEs of the composite blocks in the through-thickness direction are also compared with the values of individual constituents, that of 2D C–C compos-

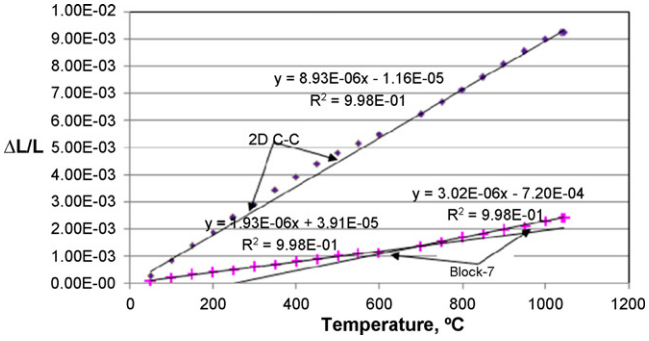

Fig. 10. Comparison of CTE of block-7 and 2D C–C composite.

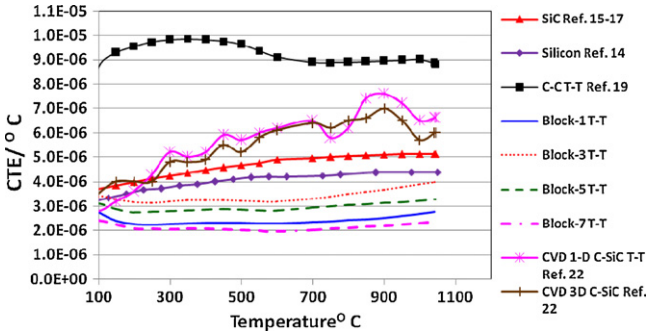

Fig. 11. Relationship between through-thickness CTE and temperature.

ite (T-T), and with the value of CVD based C–SiC composites (Fig. 11).

CTEs of all the composite blocks in the present study are lower ((2–4) × 10^{-6}/°C) than those of SiC, silicon, 2D C–C, LSI based bi-directional C–SiC composites ((2.5–7) × 10^{-6}/°C).[3] These are also lower than the CTE's of CVI based 3D C–SiC, 2D C–SiC, and 1D C–SiC composites.[22] However, the CTEs are higher than those for the in-plane direction.

Thermal expansion in the through-thickness direction may be attributed to one or more of the following.

(i) Porosity in the specimens: It may be noted that the porosity in b-7 is the highest and that in b-3 it the least. Also, CTE of b-3 is the highest and CTE of b-7 is the least. The micro-cracks are in the SiC matrix get generated during cooling in the siliconization process. In temperature segment-1 the expansion takes place and those micro-cracks are filled. In temperature segment-2 the cracks are already filled and expansion is observed beyond 650 °C.

(ii) With respect to the direction of the measurement, the carbon-fibers of the fabric are in the perpendicular direction while third direction carbon-fibers (two 6k tows, in 2 mm diameter) are parallel (Fig. 4a). As mentioned ear-

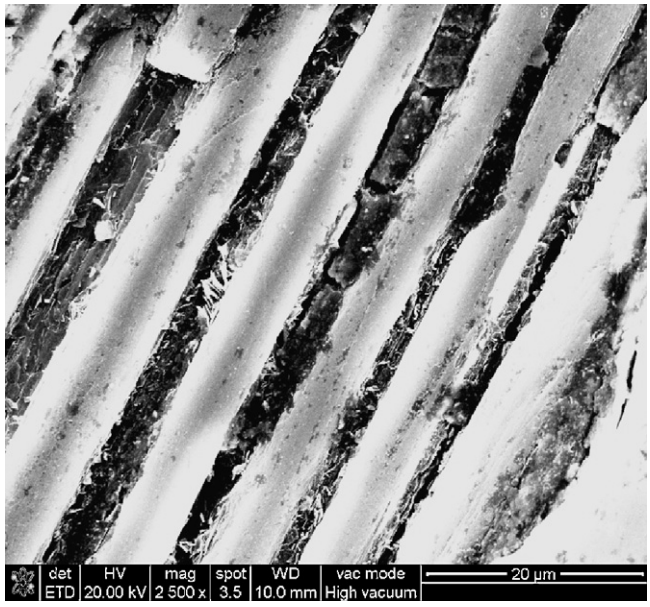

Fig. 12. Third direction fibers de-bonding after CTE measurement.

Table 2
Comparison of CTE's of C–SiC composite blocks.

C–SiC composite blocks/measurement direction	b-1	b-3	b-5	b-7	SiC	Silicon	2D C–C[19]	1D C–SiC[22]	2D C–SiC[22]
In-plane CTE/°C × 10^6									
Segment-1	−0.5	−0.5	−0.5	−0.5	4.0	3.5	0.01	4.0	4.0
Segment-2	1.16	1.12	1.23	1.12	5.0	4.0	0.02	6.0	7.0
T-T CTE/°C × 10^6									
Segment-1	2.23	3.2	2.82	1.93	4.0	3.5	9.8	5.8	5.8
Segment-2	3.68	5.48	3.99	3.02	5.0	4.0	8.8	7.8	6.9

lier, CTE along the fiber axis is much lower than the CTE in the radial direction. This mismatch in the CTE's can lead to considerable thermal stresses. When these stresses reach a critical limit, the third direction fibers may de-bond and release those stresses. For a perfectly bonded fiber–matrix interface, a micro-mechanics analysis may be applied to estimate the temperature when de-bonding is likely to take place. However, in this case such analysis is difficult to apply due to complex fiber architecture and the associated porosity in the specimens.

(iii) To understand the expansion behavior beyond 650 °C, tested specimens were observed under SEM. The SEM was focused on the third direction stitches. It appears that some of the carbon-fibers in the third direction have de-bonded from the matrix (Fig. 12). This is likely to happen when the CTE of the matrix and the radial expansion of carbon fibers are much higher than the interfacial (third direction fibers and surrounding matrix) strength. The expansion of the SiC matrix in between the fabric layers is much more pronounced than that of the third direction fibers.

Table 2 summarizes the CTE values of all the composite blocks. The through-thickness CTEs are three to four times higher than those for in-plane direction at the same siliconization conditions.

4. Concluding remarks

It is desirable to have low and uniform expansion where sudden heating induces thermal stresses. It is evident from Table 2, that the CTE is the least for the blocks which were siliconized at 1650 °C, 120 min. Also, at this condition SiC fraction was found to be the highest and residual silicon was the least. In in-plane direction the thermal expansion of the composite blocks is controlled by the warp carbon fibers, thus the effect of siliconization conditions is negligible. In through-thickness direction the thermal expansion of the composite blocks is controlled by the composition of the matrix, thus the effect of the siliconization conditions is evident. To obtain higher SiC fraction in the C–SiC composites, siliconization should be carried out at higher temperature and for longer durations.

References

1. Schulte-Fischedick, J., Zern, A., Mayer, J., Ruhle, M., Friess, M., Krenkel, W. *et al.*, The morphology of silicon carbide in C/C–SiC composites. *Mater. Sci. Eng. A*, 2002, **332**, 146–152.
2. Krenkel, W., Carbon fiber reinforced CMC for high performance structures. *Int. J. Appl. Ceram. Technol.*, 2004, **1**, 188–200.
3. Narottam, B. P., *Hand Book of Ceramic Composites*. Kluwer Acadamic Publishers, 2005, pp. 117–27.
4. Krenkel, W., Bernhard, H. and Rolpd, R., C/C–SiC composites for advanced friction systems. *Adv. Eng. Mater.*, 2002, **4**, 427–436.
5. Kochendorfer, R., Low cost processing for C/C–SiC composite by means of liquid silicon infiltration. *Ceram. Soc. Jpn.*, 1999, **3**, 451–456.
6. Kumar, S., Kumar, A., Shukla, A., Devi, R. and Ashok, K. G., Effect of carbon preform density on processing and properties of liquid silicon infiltrated C–SiC composites. In *Proceedings of the 6th International Conference on High Temperature Ceramic Composites*, 2007 [Published on CDROM].
7. Shin, D. W., Park, S. S., Choa, Y. H. and Niihara, K., Silicon/silicon carbide composites fabricated by infiltration of silicon melt into charcoal. *J. Am. Ceram. Soc.*, 1999, **82**, 3251–3253.
8. Baxter, R. I., Rawlings, R. D., Iwashita, N. and Sawada, Y., Effect of chemical vapor infiltration on erosion and thermal properties of porous carbon/carbon composite thermal insulation. *Carbon*, 2000, **38**, 441–449.
9. Gern, F. H. and Kochendorfer, R., Liquid silicon infiltration description of infiltration dynamics and silicon carbide formation. *Composites A*, 1997, **28A**, 355–364.
10. Suresh, K., Anil, K., Anupam, S., Ashok, K. G. and Rohini, D. G., Thermal-diffusivity measurement of 3D-stitched C–SiC composites. *J. Eur. Ceram. Soc.*, 2009, **29**, 489–495.
11. Fitzer, E. and Gadow, R., Fibre-reinforced silicon carbide. *Am. Ceram. Soc. Bull.*, 1986, **65**(2), 326–335.
12. Pampuch, R., Walasek, E. and Bialoskorski, J., Reaction mechanism in carbon–liquid silicon systems at elevated temperature. *Ceram. Int.*, 1986, **12**, 99–106.
13. Einset, E. O., Capillary infiltration rates into porous media with applications to silicomp processing. *J. Am. Ceram. Soc.*, 1996, **79**, 333–338.
14. Okada, Y. and Tokumaru, Y., Precise determination of lattice conditions and thermal expansion of silicon between 300 and 1500 K. *J. Appl. Phys.*, 1984, **56**(2), 314–320.
15. Nilsson, O., Harald, M., Horn, R., Jochen, F., Hofmann, R., Muller, S. G. *et al.*, Determination of the thermal diffusivity and conductivity of monocrystalline silicon carbide (300–2300K). *High Temp. High Press.*, 1997, **29**(1), 73–79.
16. Munro, R. G., Material properties of sintered α-SiC. *J. Phys. Chem. Ref. Data*, 1997, **26**(5), 1195–1203.
17. NIST, Materials properties databases for advanced ceramics. *J. Res. Natl. Inst. Stand. Technol.*, 2001, **106**, 1045–1050.
18. Li, Z. and Bradt, R. C., Thermal expansion of the cubic (3C) polytype of SiC. *J. Mater. Sci.*, 1986, **21**, 4366–4368.
19. Sinnur, K. H. *ASL/HTCC/brake-disc/2D C–C/B20*, January; 2007. Unpublished research.
20. Jian-guo, Z., Ke-zhi, L., He-jun, L., Chuang, W. and Yan-qiang, Z., The thermal expansion of carbon/carbon composites from room temperature to 1400 °C. *J. Mater. Sci.*, 2006, **41**, 8356–8358.
21. Ozbek, S., Jenkins, G. M. and Issac, D. H., Thermal expansion and creep of carbon fibers. In *Proceedings of the 20th Biennial Conf on Carbon, Amer. Ceram. Soc.*, 1991, pp. 1270–1271.
22. Zhang, Q., Laifei, C., Zhang, L. and Xu, Y., Thermal expansion behavior of carbon fiber reinforced chemical-vapor-infiltrated silicon carbide composites from room temperature to 1400 °C. *Mater. Lett.*, 2006, **60**, 3245–3247.